Cancer Chemother Pharmacol (1993) 32: 301–309

Cancer Chemotherapy and Pharmacology

Epirubicin metabolism and pharmacokinetics after conventional- and high-dose intravenous administration: a cross-over study

Carlo M. Camaggi[1], Elena Strocchi[1], Patrizia Carisi[1], Andrea Martoni[2], Barbara Melotti[2], Franco Pannuti[2]

[1] Department of Organic Chemistry, University of Bologna, Viale Risorgimento 4, I-40136 Bologna, Italy
[2] Division of Oncology, M. Malpighi Hospital, Via Albertoni 15, Bologna, Italy

Received 7 October 1992/Accepted 1 February 1993

Abstract. In a pharmacokinetics study, six patients were treated i.v. with epirubicin (EPI) at the two dose levels of 60 and 120 mg/m^2, whereas a further six patients were treated at 75 and 150 mg/m^2. Both groups were studied according to a balanced cross-over design; the aim of the study was to assess the pharmacokinetic linearity of epirubicin given at high doses. Both the absolute goodness of fit and the Akaike Information Criterion (AIC) point to a linear, tricompartmental open model as the choice framework for discussing EPI plasma disposition after 16/24 administrations, independent of the delivered dose. After 8 treatments, the minimal AIC value corresponded to a nonlinear tissue-binding model. However, even in these cases, second-order effects were present only during the early minutes following treatment. In a model-independent framework, mean EPI plasma clearance was identical at the two dose levels of 60 and 120 mg/m^2 (65.4 ± 8.0 vs 65.3 ± 13.4 l/h, $P = 0.92$). Both the mean residence time (MRT) and the volume of distribution at steady-state (V_{ss}) were similar as well (MRT: 22.6 ± 2.9 vs 24.2 ± 3.7 h; $P = 0.46$; V_{ss}: 21.3 ± 1.5 vs 22.6 ± 6.5 l/kg, $P = 0.46$). No statistically significant difference could be found in mean statistical-moment-theory parameters determined after 75- and 150-mg/m^2 EPI doses (plasma clearance, PlCl: 83.4 ± 13.5 vs 68.5 ± 12.8 l/h, $P = 0.12$; MRT: 22.6 ± 4.8 vs 21.9 ± 3.9 h, $P = 0.60$; V_{ss}: 26.7 ± 10.5 vs 21.2 ± 7.0 l/kg, $P = 0.17$). Analysis of variance also failed to reveal any significant correlation between dose and plasma clearance. However, when data relative to single patients were examined, a trend toward nonlinear drug distribution as well as a consequent increase in peripheral bioavailability could be observed in 4/6 patients of the 75-mg/m^2 vs the 150-mg/m^2 group. No significant dose-dependent variation was observed in the ratio between the molecular-weight-corrected areas under the concentration-time curve for the metabolites and those for EPI [60 vs 120 mg/m^2: epirubicinol (EPIol), 0.23 ± 0.10 vs 0.22 ± 0.06, $P = 0.20$; epirubicin glucoronide (G1), 0.46 ± 0.14 vs 0.62 ± 0.40, $P = 0.26$; epirubicinol glucuronide (G2), 0.21 ± 0.05 vs 0.30 ± 0.16, $P = 0.06$; and 75 vs 150 mg/m^2: EPIol, 0.33 ± 0.22 vs 0.32 ± 0.19, $P = 0.42$; G1, 0.51 ± 0.23 vs 0.46 ± 0.17, $P = 0.53$; G2, 0.18 ± 0.10 vs 0.22 ± 0.10, $P = 0.34$]. In conclusion, all the metabolic pathways seemed well preserved when the dose was doubled, and no evident sign of "saturation kinetics" could be found.

Introduction

The new anthracycline antibiotic epirubicin (4′-epidoxorubicin, EPI) differs from doxorubicin (DX) in the epimerization of the OH group in position 4′ of the aminosugar moiety. Preclinical studies in animal models and extensive clinical trials have proven that this compound is less toxic than DX at similar equipotent therapeutic doses [13, 15, 27, 28]. DX and EPI are significantly metabolized in cancer patients. Both drugs are reduced to the 13-hydroxy derivatives doxorubicinol (DXol) and epirubicinol (EPIol), respectively. In all patients, DXol is the main DX metabolite in both plasma and urine. Compounds lacking the aminosugar moiety can also be detected for both drugs. An additional metabolic pathway is possible for EPI. Conjugation with glucuronic acid takes place at the oxydryl group in position 4′ of the aminosugar; the glucuronide 4′-*O*-β-D-glucuronyl-4′-EPI (metabolite G1) and 4′-*O*-β-D-glucuronyl 13-dihydro-4′-EPI (metabolite G2) represent the majority of the EPI-derived circulating species [3, 5, 7, 20, 22, 25]. The main pharmacokinetic consequence of this additional EPI detoxication route is a more efficient and faster elimination of the unchanged drug as compared with DX, as demonstrated by the statistically significant differences between the two compounds in terms of the area under the concentration-time curve (AUC), plasma clear-

Correspondence to: C. M. Camaggi

Table 1. Characteristics of the patients and detail of treatments

Patient number	Tumor	Age (years)	Weight (kg)	Height (cm)	Perf.Stat. (WHO)	Low-dose treatment			High-dose treatment		
						Line[a]	Dose (mg)	Infusion time (min)	Line[a]	Dose (mg)	Infusion time (min)
1	Lung	62	78.5	166	1	2	110	7.50	1	225	6.75
5	Lung	49	59.3	170	1	1	100	4.00	2	220	6.00
6	Lung	63	79.0	169	0	1	110	4.00	2	220	9.50
8	Lung	64	67.0	168	1	1	105	4.08	2	210	9.67
10	Lung	61	61.2	170	1	2	100	6.25	1	200	9.00
11	Lung	37	61.8	170	1	2	100	2.92	1	200	6.92
2	Lung	64	81.5	177	1	1	150	6.00	2	300	10.00
3	UNK	59	78.0	174	1	1	150	5.50	2	280	13.00
4	UNK	41	77.0	179	1	2	140	4.50	1	280	10.50
7	Lung	67	78.0	170	1	2	145	5.92	1	280	9.00
9	Lung	64	71.2	175	1	2	135	4.17	1	280	10.33
12	Lung	50	54.7	171	1	1	125	3.83	2	240	7.83

[a] Line 1, first treatment; line 2, second treatment
Perf. stat., Performance status; UNK, Unknown primary

ance (PlCl), mean residence time (MRT), and half-life ($t_{1/2}$) of the slow disposition phase [5, 11].

The lower toxicity of this new analog when it is given at the same dose as DX appears to be related to the above-mentioned pharmacokinetic factors rather than to a different mode of action. This behavior has prompted several clinical trials that have investigated the feasibility and efficacy of high-dose EPI therapy; obviously, it is worth trading off the lower toxicity of the new anthracycline with its increased efficacy.

We report the results of a pharmacokinetics study in which six patients were treated with EPI at the two dose levels of 60 and 120 mg/m^2, whereas another group of six patients were treated at 75 and 150 mg/m^2. Both groups were studied according to a balanced cross-over design. The aim of our study was to assess the linearity in the pharmacokinetics of EPI given at "high" doses. The data presented support the conclusion that a linear, compartmental pharmacokinetic model can adequately explain EPI plasma disposition. The best nonlinear kinetic model capable of approximating EPI plasma concentrations is also described. Finally, plasma concentrations of both EPI and its metabolites are discussed within a model-independent framework to see how dose variations influence EPI elimination, distribution, and biotransformation.

Patients and methods

Patients

A total of 12 inpatients with advanced cancer were included in this study, which was conducted at the Division of Oncology, M. Malpighi Hospital, Bologna, Italy, during a phase I study for the evaluation of epirubicin given at high doses. All patients gave their informed consent to participate in the study. After pharmacokinetic evaluation, the patients who entered the study continued the treatment with epirubicin as long as was medically required.

The eligibility criteria were:

A. Progressive neoplastic disease not previously treated with chemotherapy
B. A life expectancy of >3 months
C. A performance status of 0, 1, or 2 according to the WHO scale
D. A WBC count of >4,000/mm^3 and a platelet count of >120,000/mm^3
E. Creatinine clearance of >60 ml/min
F. A total bilirubin level of <1.2 mg/100 ml, SGOT and SGPT values of <45 mU/ml, and an alkaline phosphatase level of <130 mU/ml
G. Informed consent

The exclusion criteria were:

A. The presence of cardiac disorders
B. The presence of documented liver metastases with or without hepatic dysfunction (a total bilirubin level of >1.2 mg/100 ml and/or SGOT and SGPT values of >45 mU/ml and/or an alkaline phosphatase level of >130 mU/ml)
C. A previous episode of severe drug allergy
D. Mentally incapacitated subjects

Each patient was treated at two EPI dose levels: 60 and 120 mg/m^2 or 75 and 150 mg/m^2. The treatment was assigned according to a randomized, balanced cross-over design.

The patients' characteristics and the treatment details are reported in Table 1.

EPI was given as a constant-rate, rapid intravenous (i.v.) infusion (Farmorubicina, lyophylized powder for i.v. injection, 50-mg vials). The infusion time was always recorded exactly (Table 1). Blood samples were drawn before treatment and at 0 (i.e., immediately after the i.v. infusion), 5, 15, 30, and 60 min and 2, 4, 8, 12, 24, 36, 48, 72, 96, 120, 144, and 168 h after drug administration. Plasma separated by centrifugation was kept frozen at –20° C in light-protected tubes; drug and metabolite analysis was performed no later than 48 h after sampling.

Analytical methods

A high-performance liquid chromatographic (HPLC) assay with fluorimetric detection was applied for the quantitative determination of EPI and its known fluorescent metabolites. The method was specific for the simultaneous assay of unchanged drug, epirubicinol (EPIol), 7-deoxy-Adriamycinone (metabolite C), Adriamycinone (metabolite D), 7-deoxy-13-dihydro-Adriamycinone (metabolite E), 13-dihydro-Adriamycinone (metabolite F), 4′-*O*-β-D-glucuronyl-4′-EPI (metabolite G1), and 4′-*O*-β-D-glucuronyl-13-dihydro-4′-EPI (metabolite G2). A detailed description of the analytical method has been published elsewhere [4].

Pharmacokinetic analysis

A model-independent pharmacokinetic analysis, a compartmental model, and a nonlinear tissue-binding model were adopted for the interpretation of plasma disposition kinetics.

Linear compartmental model. As shown by Manaka et al. [18], the three-compartment open-model with elimination from a peripheral compartment (called the "first-pass" model and often used in disposition kinetics studies) is not globally identifiable, i. e., a given set of input-output data does not uniquely identify a single parametrization vector. A tricompartmental openmodel with elimination from the central compartment does not present this problem and was therefore preferred in our computations according to the principle of parsimony in model building and to the Akaike Information Criterion (AIC).

Plasma EPI concentrations were computer-fitted to the differential-equation system:

$$dx_1/dt = -(k_{12}+k_{13}+k_{el})x_1+k_{21}\,x_2+k_{31}\,x_3+k_0u$$
$$dx_2/dt = k_{12}x_1-k_{21}\,x_2$$
$$dx_3/dt = k_{13}x_1-k_{31}\,x_3,$$

with zero initial state:

$$x_1(t=0) = 0;\ x_2(t=0) = 0;\ x_3(t=0) = 0 \text{ and}$$
$$c_1 = x_1/v_1,$$

where x_1, x_2, and x_3 are the amounts of drug in compartments 1, 2, and 3, respectively; k_0 is the zero-order infusion rate (set equal to zero in the postinfusion decay phase); u is the delivered dose, c_1 is the EPI concentration in compartment 1; and v_1 is the apparent volume of compartment 1.

Nonlinear model. A nonlinear tissue-binding model [24], modified to take into account the non-zero infusion time, was also tested. In linear models, it is accepted that drugs interact with "tissues" present in superabundance; the fraction bound in tissues at steady-state is therefore essentially constant and independent of the drug concentration. The nonlinear tissue-binding model used in this work to describe EPI disposition removes the pseudo-first-order assumption and lets EPI compete with a limited amount of binding sites.

EPI plasma concentrations [EPI] were computer-fitted to the differential-equation system:

$$d[EPI]/dt = -(k_1[EPI][T]+k_{el}[EPI]) + k_2[EPI.T] + k_0/v$$
$$d[EPI.T]/dt = -k_2[EPI.T] + k_1[EPI][T],$$

with
$[EPI]_{t=0} = 0$,
$[T]_{t=0} = T_{0/v}$,
$[EPI.T]_{t=0} = 0$, and
$[T] = T_0/v - [EPI.T]$,

corresponding to the kinetic scheme:

$$EPI + T \underset{k_2}{\overset{k_1}{\rightleftharpoons}} EPI.T$$

$$EPI \xrightarrow{k_{el}} \text{Metabolites + Excretion},$$

with zero-order EPI infusion (at a rate k_0) in a system of apparent volume v containing an amount T_0 of "tissue." The term "tissue" (or "binding site") is used herein to indicate any species capable of reversibly binding EPI. The complex EPI.tissue that is formed constitutes a new species not measured as EPI in the analytical assay.

Several more complex models can be easily depicted and numerically solved. However, checks following the AIC have indicated that any increase in the number of independent parameters runs counter to the principle of parsimony in modelbuilding.

Minimization procedure and model selection. Nonlinear fitting of the experimental data points to a mathematical model was performed with specifically designed double-precision FORTRAN programs based on the CERN MINUIT package [17]. Kinetic microconstants (and errors) were directly determined by interfacing a numerical differential-equation solver (Runge-Kutta algorithm) with the minimization package. Experimental uncertainties on concentration data were explicitly taken into account by weighting the chi-square error function F as described elsewhere [6, 9, 10, 17]. The selection of the mathematical model describing the drug and metabolite concentration-time course was performed according to the AIC, which is a mathematical formulation of the principle of parsimony in model building [1, 26].

Model-independent parameters. The experimental data were analyzed according to statistical moment theory [14], which requires the evaluation of the area under the concentration-time curve (AUC) and the area under the concentrationxtime-time curve (AUMC). Although these data could be computed according to the trapezoidal rule, a better approximation to AUC, AUMC, and $t_{1/2}$ values (as well as to 1 SD errors on these parameters) can be obtained with interpolation procedures [5, 6].

Experimental concentrations (C) of EPI, EPIol, glucuronide G1, and glucuronide G2 measured over the 0- to 168-h interval were therefore computed-fitted with a linear combination of exponential terms:

$$C = \sum_{i=1}^{n} A_i \exp(-a_i(t-\tau)),$$

with:

$$\sum_{i=1}^{n} A_i = C_0.$$

For EPI, τ, representing the time lag for the appearance of the product in plasma, was always fixed at zero.

The time of infusion (t_{inf}) was also taken into account. The corrected A'_i preexponential terms [12] were computed according to the formula:

$$A_i = \frac{A_i a_i t_{inf}}{1 - e^{(-a_i t_{inf})}},$$

and AUC and AUMC were then computed as usual:

$$AUC = \sum_{i=1}^{n} \frac{A_i}{a_i}\ ;\ AUMC = \sum_{i=1}^{n} \frac{A_i}{a_i^2}$$

The mean residence time (MRT, corrected for the input mean transit time) was obtained [21] as:

$$MRT = \frac{AUMC}{AUC} - \frac{t_{inf}}{2}.$$

Plasma clearance (PlCl) and the volume of distribution at steady-state (V_{ss}) were calculated as usual [14, 21]. Metabolite AUC and AUMC values were computed according to the trapezoidal rule and/or from the interpolation equation, with no correction for infusion time.

Error analysis. In a cross-over experiment, in which intrasubject data are compared, the only way to state with statistical significance whether parameter q differs between the two measurements in the *same patient* is to take the experimental error into account [6]. Errors on pharmacokinetic parameters were computed according to standard error-propagation rules [2]:

$$\Delta q = \sqrt{\left(\frac{\delta q}{\delta x}\Delta x\right)^2 + \ldots + \left(\frac{\delta q}{\delta z}\Delta z\right)^2},$$

starting from the parameter errors computed in the interpolation procedure, and represent 1 SD errors.

When relevant, a z-test [2] was performed to check whether corresponding parameters were identical within the experimental error ($P = 0.05$) as measured after conventional- and high-dose treatment *in the same patient*. Differences outside the experimental error are asterisk-flagged in the tables.

Group comparison was performed with the BMDP package [8] according to the Wilcoxon signed-rank test (the nonparametric analog of a matched-pairs t-test), the Mann-Whitney rank-sum test (the non-para-

Table 2. Low- versus high-dose EPI administration: half-lives of the three decay phases

	$t_{1/2a1}$		$t_{1/2a2}$		$t_{1/2a3}$	
Patient	60 mg/m²	120 mg/m²	60 mg/m²	120 mg/m²	60 mg/m²	120 mg/m²
1	4.13 ± 0.23	3.71 ± 0.19	3.08 ± 0.52	2.87 ± 0.78	37.2 ± 1.5	33.8 ± 1.4
5	2.80 ± 0.13	3.08 ± 0.12	7.67 ± 0.61*	3.66 ± 0.76*	53.0 ± 5.5*	38.8 ± 2.1*
6	3.51 ± 0.21	3.96 ± 0.25	0.53 ± 0.10*	1.62 ± 0.40*	30.7 ± 0.9*	33.6 ± 1.1*
8	3.31 ± 0.16*	4.01 ± 0.21*	2.39 ± 0.33*	4.87 ± 0.72*	32.4 ± 1.4*	38.0 ± 2.0*
10	2.60 ± 0.13*	3.33 ± 0.24*	0.71 ± 0.15	1.03 ± 0.18	28.5 ± 0.9	29.0 ± 0.8
11	2.50 ± 0.12*	1.73 ± 0.31*	3.67 ± 0.80*	0.15 ± 0.04*	30.3 ± 1.0	28.8 ± 0.7
Mean	3.14 min	3.30 min	3.01 h	2.37 h	35.34 h	33.67 h
SD	0.63	0.85	2.60	1.76	9.13	4.26
	$t_{1/2a1}$		$t_{1/2a2}$		$t_{1/2a3}$	
	75 mg/m²	150 mg/m²	75 mg/m²	150 mg/m²	75 mg/m²	150 mg/m²
2	3.28 ± 0.19	3.43 ± 0.28	0.88 ± 0.23	0.33 ± 0.31	23.0 ± 0.6*	20.9 ± 0.3*
3	3.15 ± 0.18	3.60 ± 0.27	1.96 ± 0.35	1.78 ± 0.21	29.0 ± 1.1	28.1 ± 0.8
4	2.83 ± 0.25	3.28 ± 0.23	1.03 ± 0.10	1.35 ± 0.19	33.7 ± 1.1	35.6 ± 1.7
7	3.29 ± 0.16	2.87 ± 0.21	7.72 ± 1.04*	1.41 ± 0.38*	35.7 ± 2.5	35.5 ± 1.7
9	4.10 ± 0.30*	2.90 ± 0.18*	3.15 ± 0.49*	5.33 ± 0.58*	36.3 ± 1.5	35.8 ± 1.9
12	2.73 ± 0.15	2.96 ± 0.18	3.93 ± 0.57*	1.12 ± 0.30*	34.9 ± 1.7	30.8 ± 1.4
Mean	3.23 min	3.17 min	3.11 h	1.89 h	32.10 h	31.12 h
SD	0.48	0.30	2.55	1.76	5.19	5.93

* Data significantly different as measured after low- vs high-dose administration in the same patient

metric version of the two-sample *t*-test), and the Kruskal-Wallis test (corresponding to one-way analysis of variance). Only the Wilcoxon test is cited in the discussion in cases for which the tests gave equivalent results.

Results

The best fit (according to the AIC) to the plasma concentration-time course of EPI after i.v. treatment was obtained for all the patients by a triexponential equation. The results of the biexponential analysis are not reported herein because in all cases, the fit with the experiment was rather poor.

The mean half-lives of the three exponential decay phases (Table 2) were similar at all dose levels, and on the whole, no statistically significant difference could be found. Two subjects (patients 6 and 8) showed a limited but significant (i.e., outside experimental uncertainty) increase (+11.6% and +6.8%) in terminal half-life when the dose was increased (from 60 to 120 mg/m²). In contrast, patients 2 and 5 showed a significant decrease in terminal half-life when the dose was doubled. Of the 12 patients, 7 showed a significant variation in a_2 half-life, but no definite trend toward an increased or decreased value could be found. Similarly, in 2/12 patients the value for $t_{1/2a1}$ rose significantly with the dose, whereas in 2/12 subjects a reversed effect was observed.

Figure 1 reports the relative AIC values $[(AIC_l - AIC_{nl})/AIC_l]$ obtained by fitting the tricompartmental linear model (AIC_l) and the nonlinear tissue-binding model (AIC_{nl}) to the experimental EPI concentrations. Negative values indicate a better agreement of the experiment with the linear model.

In each case, the covariance matrix at the minimum was positive-definite and a satisfactory error estimation could be carried out. The minimal F values found in the minimization procedure using Runge-Kutta integration of the differential equation system relative to the tricompartmental open model were quite close to the corresponding values obtained in the triexponential interpolation, as theoretically expected. As a check of goodness-of-fit, parameters of the triexponential equation can also be back-computed from the kinetic microconstants of the linear model [24]; the agreement is within the experimental error.

Some intrasubject variability of kinetic parameters could be observed after two consecutive administrations, but no statistically significant difference related to the delivered dose was found. In particular, the kinetic constant k_{el}, describing all irreversible processes resulting in the elimination of EPI from the sampling compartment, was remarkably stable at all dose levels (Table 3). As in the linear case, the kinetic constant k_{el} computed for the nonlinear tissue-binding model did not significantly depend on the delivered dose (k_{el}: 60 mg/m², 8.64 ± 2.34 h^{-1}; 120 mg/m², 7.23 ± 3.28 h^{-1}, $P_{60-120} = 0.46$; 75 mg/m², 8.83 ± 3.69 h^{-1}; 150 mg/m², 8.01 ± 2.81 h^{-1}, $P_{75-150} = 0.46$).

The statistical-moment-theory parameters (calculated from the coefficients of the triexponential equation) are reported in Table 4 together with their 1 SD errors. Mean EPI plasma clearance was identical at the two dose levels of 60 and 120 mg/m² ($P = 0.92$). Only patient 10 showed a significant variation in this parameter. Both the MRT and the V_{ss} values were similar as well (MRT, $P = 0.46$; V_{ss},

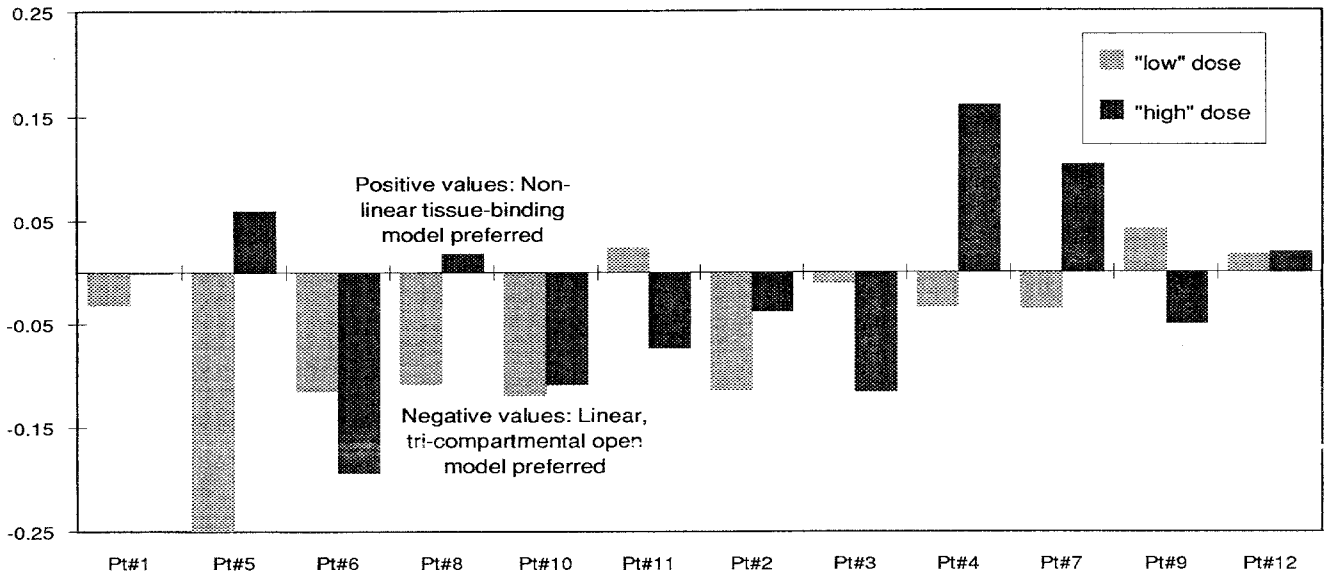

Fig. 1. Relative AIC values ($[AIC_l - AIC_{nl}]/AIC_l$) obtained by fitting the tricompartimental linear model (AIC_l) and the nonlinear tissue-binding model (AIC_{nl}) to the experimental EPI concentrations. Negative values indicate a better agreement of the experiment with the linear model

Table 3. Kinetic microconstants, linear model

	60 mg/m²	120 mg/m²	75 mg/m²	150 mg/m²
k_{12} (h^{-1})	3.5 ± 2.7	2.4 ± 0.8	4.5 ± 1.9	3.8 ± 2.0
k_{21} (h^{-1})	0.6 ± 0.5	1.2 ± 2.1	0.6 ± 0.4	0.8 ± 0.7
k_{13} (h^{-1})	4.4 ± 1.9	5.7 ± 3.9	3.7 ± 1.5	4.8 ± 2.1
k_{31} (h^{-1})	0.04 ± 0.01	0.05 ± 0.02	0.04 ± 0.01	0.05 ± 0.03
k_{el} (h^{-1})	5.6 ± 1.2	5.3 ± 1.3	4.7 ± 1.3	5.0 ± 0.9
V_c (l)	12.0 ± 2.4	13.0 ± 4.4	19.4 ± 8.7	14.1 ± 3.8

Data represent mean values ± SD

Table 4. High-dose EPI administration: model-independent parameters

	PlCl		MRT		V_{ss}	
Patient	60 mg/m²	120 mg/m²	60 mg/m²	120 mg/m²	60 mg/m²	120 mg/m²
1	70.0 ± 4.6	60.0 ± 4.3	24.3 ± 2.4	20.7 ± 1.9	21.6 ± 3.5	15.8 ± 2.6
5	50.2 ± 3.8	52.9 ± 3.7	27.1 ± 4.3	20.6 ± 2.1	22.9 ± 5.4	16.3 ± 2.8
6	66.9 ± 3.8	56.9 ± 3.6	23.7 ± 1.8*	29.3 ± 2.2*	20.0 ± 2.6	20.6 ± 2.9
8	67.4 ± 4.3	65.9 ± 4.8	19.4 ± 1.9	23.2 ± 2.5	19.5 ± 3.1	21.9 ± 3.9
10	73.3 ± 4.3*	90.8 ± 5.9*	21.0 ± 1.7	23.0 ± 1.8	23.3 ± 3.2	31.2 ± 4.5
11	64.8 ± 4.5	65.0 ± 5.3	20.2 ± 2.0*	28.2 ± 2.5*	20.7 ± 3.5	29.7 ± 5.1
Mean	65.4 l/h	65.3 l/h	22.6 h	24.2 h	21.3 l/kg	22.6 l/kg
SD	8.0	13.4	2.9	3.7	1.5	6.5

	PlCl		MRT		V_{ss}	
	75 mg/m²	150 mg/m²	75 mg/m²	150 mg/m²	75 mg/m²	150 mg/m²
2	85.1 ± 5.2*	55.5 ± 3.1*	18.2 ± 1.4	20.3 ± 1.3	19.0 ± 2.6	13.6 ± 1.6
3	92.9 ± 6.7*	58.5 ± 4.5*	16.5 ± 1.7	15.4 ± 1.4	19.7 ± 3.4*	11.4 ± 1.9*
4	77.1 ± 4.9	89.6 ± 6.6	24.5 ± 2.1	24.4 ± 2.4	24.9 ± 3.7	28.4 ± 4.9
7	63.6 ± 5.6	68.9 ± 5.7	21.1 ± 3.3	26.9 ± 2.8	17.2 ± 4.2	23.7 ± 4.4
9	102.6 ± 7.3*	76.7 ± 5.8*	28.6 ± 3.0	21.9 ± 2.5	41.3 ± 7.2*	24.1 ± 4.5*
12	79.1 ± 5.6*	61.8 ± 4.5*	26.5 ± 2.8	22.2 ± 2.0	38.3 ± 6.7	26.2 ± 4.3
Mean	83.4 l/h	68.5 l/h	22.6 h	21.9 h	26.7 l/kg	21.2 l/kg
SD	13.5	12.8	4.8	3.9	10.5	7.0

* Data significantly different as measured after low- vs high-dose administration in the same patient

Table 5. EPI glucuronide, mean pharmacokinetic parameters ± SD

	60 mg/m²	120 mg/m²	75 mg/m²	150 mg/m²
$t_{1/2a1}$ (h)	0.66 ± 0.24	0.65 ± 0.18	0.47 ± 0.12	0.54 ± 0.49
$t_{1/2a2}$ (h)	1.43 ± 0.30	1.71 ± 0.54	1.64 ± 0.66	2.55 ± 1.92
$t_{1/2a3}$ (h)	20.3 ± 5.1	23.1 ± 4.0	25.0 ± 4.8	27.9 ± 8.6
Time delay (h)	0.081 ± 0.063	0.072 ± 0.045	0.065 ± 0.035	0.029 ± 0.060
Time to peak (h)	1.47 ± 0.37	1.54 ± 0.20	1.27 ± 0.34	1.23 ± 0.77
C_{max} (ng/ml)	163 ± 63	317 ± 140	200 ± 111	322 ± 187

Table 6. EPIol glucuronide, mean pharmacokinetic parameters ± SD

	60 mg/m²	120 mg/m²	75 mg/m²	150 mg/m²
$t_{1/2a1}$ (h)	1.15 ± 0.49	1.23 ± 0.27	0.76 ± 0.41	1.1 ± 0.40
$t_{1/2a2}$ (h)	2.00 ± 1.04	1.77 ± 0.50	2.04 ± 0.68	2.36 ± 1.69
$t_{1/2a3}$ (h)	20.80 ± 2.9	21.5 ± 2.7	24.1 ± 7.7	24.1 ± 8.7
Time delay (h)	0.17 ± 0.08	0.15 ± 0.09	0.16 ± 0.05	0.18 ± 0.14
Time to peak (h)	2.25 ± 0.64	2.42 ± 0.41	1.92 ± 0.81	2.39 ± 0.69
C_{max} (ng/ml)	50 ± 18	104 ± 44	44 ± 25	104 ± 50

Table 7. Molecular-weight-corrected AUC values for the parent drug and its metabolites

	60 mg/m²	120 mg/m²	75 mg/m²	150 mg/m²
EPI	2966 ± 382	6203 ± 1298	3179 ± 593	7640 ± 1505
EPIol	664 ± 292	1334 ± 423	1027 ± 685	2481 ± 1927
Glucuronide G1	1298 ± 339	3401 ± 1878	1590 ± 843	3313 ± 1288
Glucuronide G2	623 ± 172	1654 ± 664	578 ± 391	1540 ± 735
Aglycone C	687 ± 546	1640 ± 1280	784 ± 895	1802 ± 1073
Aglycone D	301 ± 538	539 ± 609	492 ± 916	1142 ± 1854
Aglycone E	985 ± 458	2413 ± 1723	786 ± 1290	1873 ± 1830
Aglycone F	112 ± 118	371 ± 348	104 ± 141	297 ± 224

Data represent mean values ± SD (expressed in pmol h ml^{-1})

$P = 0.46$). Therefore, at a macroscopic level, no differences are found in EPI elimination and distribution when the dose is increased from 60 to 120 mg/m². No statistically significant difference could be found either in mean statistical-moment-theory parameters determined after 75- and 150-mg/m² EPI doses (PlCl, $P = 0.12$; MRT, $P = 0.60$; V_{ss}, $P = 0.17$). Analysis of variance (ANOVA) also failed to reveal any significant correlation between dose and plasma clearance at these two dose levels (regression, $P = 0.085$, $r^2 = 0.194$; i.e., only 19.4% of the variability in PlCl is explained by correlation with the delivered dose). When ANOVA was performed taking into account all four dose levels, only about 1% of the variability in plasma clearance was found to be related to the delivered dose. Conversely, the relationship between the delivered dose and the EPI AUC was highly significant ($P = 0.007$; $r^2 = 0.986$).

The EPI metabolic pathways observed in this study are consistent with those previously reported in the literature by us and by other authors [3, 5, 7, 22, 25]. Four main biotransformation routes can be observed: (1) reduction of the C-13 keto group with the formation of EPIol, (2) conjugation with glucuronic acid with the formation of 4′-*O*-β-D-glucuronyl-4′-EPI (metabolite G1), (3) loss of the aminosugar moiety through a hydrolytic process with the formation of the aglycone Adriamycinone (metabolite D), and (4) loss of the aminosugar moiety through a redox process with the formation of the deoxyaglycone 7-deoxy-Adriamycinone (metabolite C). EPIol formed through biotransformation 1 can also follow metabolic routes 2, 3, and 4 with the formation of metabolites 4′-*O*-β-D-glucuronyl-13-dihydro-4′-EPI (metabolite G2), 13-dihydro-Adriamycinone (metabolite F), and 7-deoxy-13-dihydro-Adriamycinone (metabolite E), respectively.

The glucuronide G1 and G2 plasma concentration-time course can be well simulated by a triexponential equation with $A_1 = -(A_2 + A_3)$ and a time-delay τ. The mean values obtained for the half-lives of the input phase a_1, and of the two decay phases a_2 and a_3, for the time delay τ, for the time to peak, and for C_{max} (computed by putting equal to zero the first derivative of the plasma concentration curve) are reported in Tables 5 and 6 for EPI glucuronide and EPIol glucuronide, respectively.

A difference in behavior can be observed between the plasma concentration-time courses of EPIol and glucuronide G1, both of which are formed directly from EPI. Metabolite G1 is characterized by a well-defined triphasic concentration-time curve with a time delay of 0–10 min before its appearance in plasma, followed by a rapid increase in the plasma concentration and by two decay phases with half-lives of about 1–2 and 20–30 h, respectively (Table 5). The appearance of EPIol is considerably faster, and the first decay phase is not as well defined as that in the G1 time curve. As EPIol decay is equally well

explained (in terms of the error function F) by bi- and tri-exponential equations, the less complex biexponential model was selected according to the AIC. A reliable estimation of the EPIol input half-life was possible only in two subjects (patients 6 and 7). In all other cases, only the terminal decay phase was studied ($t_{1/2}$: 60 mg/m^2, 29.4 ± 5.2 h; 120 mg/m^2, 30.2 ± 5.2 h; 75 mg/m^2, 30.8 ± 8.7 h; 150 mg/m^2, 31.2 ± 7.2 h).

The molecular weight-corrected AUC values obtained for EPI and its metabolites are shown in Table 7. Inter- and intrasubject variability was more evident in the metabolite data than in the unchanged-drug behavior. The coefficient of variation (CV) on the EPI AUC was between 13% and 21% at each dose level. The EPIol CV was 32%–78%; a similar range was observed for the CV on the AUC of glucuronic acid conjugates (26%–68%). Aglycone derivatives were nearly absent in some patients, whereas in others they represented a major metabolic pathway. These compounds are also known to be formed when plasma samples are mismanaged; this problem is well recognized in our laboratory, and care has been taken to avoid artifacts. As a rule, deoxyaglycones C and E are the main deglycosylated products found in plasma that derive from EPI and EPIol, respectively.

As in the case of the unchanged drug, mean metabolite terminal half-lives were not significantly influenced by the delivered dose. In individual patients, differences (excluding the experimental uncertainty) between terminal half-lives at the two dose levels could sometimes be detected, but no definite trend toward a $t_{1/2}$ increase or decrease with dose was found.

Discussion

The aim of this work was to discuss the "linearity" of EPI pharmacokinetics after fast i.v. infusion. This problem has recently been considered by other authors. In a paper designed to establish the maximum tolerated EPI dose, Tjuljandin et al. [23] state that ". . . interpatient variation occurred in the pharmacokinetics at each dose level but overall there were dose-dependent pharmacokinetics." The main reason for this statement was the absence of a significant linear correlation between the delivered dose and the AUC. In a study on 78 patients with metastatic breast cancer who were randomized to 4 different dose levels (40, 60, 90, and 135 mg/m^2) of EPI, Jakobsen et al. [16] instead found a significant linear correlation between the delivered dose and the AUC, notwithstanding a large interpatient variability in this pharmacokinetic parameter.

In our study, we tried to optimize the experimental detail to obtain representative results. First, we followed a randomized cross-over design to avoid interpatient variability (in both of the above-mentioned investigations, no dose escalation was undertaken in individual patients). Second, as the half-life of the EPI first decay phase is of the same order as the infusion time, the approximation of a "fast infusion" to an i.v. bolus (with all the drug being forced instantaneously into the central compartment) is not acceptable. The infusion times were therefore explicitly considered. Finally, sampling times and a nonlinear fitting procedure were selected in this work for a better estimation of the fast α-decay phase and of the long terminal half-life typical of anthracycline drugs. Omission of the t = 0 data point (relative to the sample taken immediately after drug administration in the contralateral arm) in the interpolation procedure results in very large errors in the A1 intercept. When the sampling is limited to 24 – 30 h after treatment, information on the slow terminal phase is lost. Our interpolation procedure also explicitly takes into account the analytical precision of experimental data points by weighting each concentration with its variance [6].

The triexponential decay of EPI plasma concentration after i.v. administration observed herein is in agreement with a linear, "tricompartmental" pharmacokinetic model, but not with Michaelis-Menten kinetics, which generates inward-curved semilogarithmic plasma-level plots [24]. Similar behavior has been observed by us and by other authors for related anthracycline antibiotics such as doxorubicin and idarubicin [3, 5, 6]. The selection of a triexponential equation is based on the (restrictive) AIC. Tjuljandin and co-workers [23] prefer a two-exponential equation to describe EPI disposition because ". . . the coefficient of correlation for the two-exponential parameters was in all cases slightly higher than for three exponents." In nonlinear fittings, a high "coefficient of correlation" between parameters is an indication not of good fit but rather of poor modeling [9, 10]. In most of Jakobsen et al.'s patients [16], a triexponential decay was found to be adequate according to the AIC. In our experiments, no dose-dependent variation in EPI half-lives was observed.

Deterministic, linear compartmental systems as well as nonlinear, saturation-limited models are often only rough approximations of biological reality; nevertheless, they are operationally accepted to describe drug disposition. Little physiological significance can generally be attached to the numeric values of the kinetic constants determined following these kinds of treatment; we shall not, however, discuss *every single constant* but the *model* itself. If sharp deviations from kinetic linearity are present, no linear model can describe *any single concentration decay curve* obtained at doses above the "linearity" threshold. On the contrary, a nonlinear model can collapse into a linear model if far removed from the saturation conditions and thus well describes a "linear" decay curve [19].

Both the absolute goodness of fit and the AIC point to a linear model as the choice framework for discussing EPI plasma disposition in 16/24 of our cases. The pattern of the kinetic constants is typical of drugs with a "deep" peripheral compartment. In these cases, the long terminal decay phase represents not slow metabolism or elimination but rather the balance between slow drug release from the inner compartment (described by k_{31}) and a relatively fast elimination phase (described by k_{el}).

The AIC prefers the nonlinear tissue-binding model in 8/24 cases. However, as can be observed in Fig. 2, even in the case in which the difference in AIC between the linear and the nonlinear model is greater, both models actually give a good apparent fit of the experimental data. The amount of binding sites available for complexation with

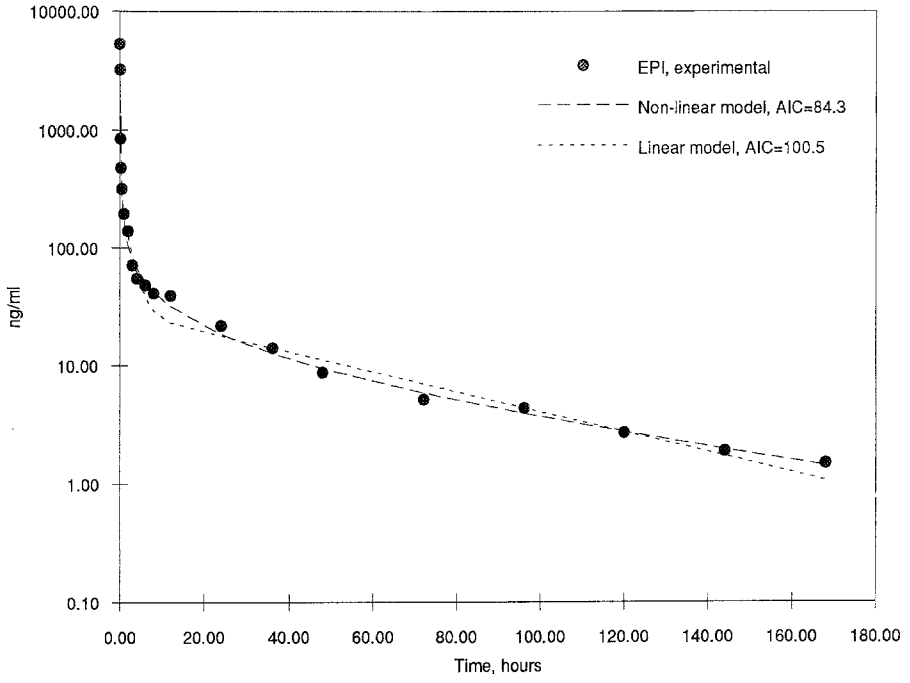

Fig. 2. Patient 7 represents the case in which the difference between the AIC obtained with the tricompartmental linear model (AIC = 100.5) and that calculated with the nonlinear tissue-binding model (AIC = 84.3) is greater. Even in this case, both models actually give a good apparent fit of the experimental data

the free drug is as a rule *in excess* of the amount of free drug, and second-order effects scarcely influence the plasma decay curve. From an operativistic point of view, it can be concluded that the deviation from linearity is of a limited degree, even in the eight treatments for which a nonlinear description must be preferred.

Clinicians are generally more concerned with macroscopic events such as bioavailability changes than with subtle model-dependent variations in kinetic microconstants. Statistical moment theory (SMT) is, in our opinion, the best framework for deriving clinically relevant information. A theoretical reservation can be raised a priori: the model-independent approach was originally developed to deal with linear systems, and some of the conclusions drawn are strictly true only if all dispositional processes can be described by first-order kinetics with the elimination occurring from the sampling system. On the other hand, we have proven that a linear model with elimination from the sampling system gives an appropriate description of the experimental data; SMT can therefore be used to derive relevant disposition parameters for each treatment.

Our study was designed to detect at an alpha level of 0.05 with power = 0.8 an average difference in EPI plasma clearance of 30% between two dose levels, estimated to be clinically significant and larger than the average intersubject variability. A straightforward examination of SMT parameters shows that mean EPI plasma clearance is identical at the two dose levels of 60 and 120 mg/m^2; the average difference of 18% between PlCl as determined after 75- and 150-mg/m^2 EPI doses is not significant under the study design. Nevertheless, it cannot be ignored that in the latter group, patients 2, 3, 9, and 12 displayed a 22%–37% decrease in plasma clearance when the delivered dose was increased to 150 mg/m^2. This variation was outside the experimental error and can be explained by distribution factors; in each patient, the decrease in PlCl was paralleled by a similar decrease in the volume of distribution at steady state.

We can therefore conclude that in our patient sample, the impact of dose on relative plasma EPI bioavailability could be observed only in individual patients at the highest (150 mg/m^2) dose level; moreover, it was of limited scope and its magnitude was similar to the random intersubject variation. When present, increased plasma bioavailability is the consequence of a reduced extraplasmatic distribution of the unchanged drug. This was the main reason why we preferred to test a nonlinear tissue-binding model instead of "Michaelis-Menten" saturation kinetics as a source of kinetic nonlinearity. It is also noteworthy that all patients who showed reduced plasma clearance at the highest dose level actually had an above-average baseline EPI clearance.

The EPI metabolic pathways observed in this study are consistent with those previously reported in the literature by us and by other authors. If EPI metabolism is controlled by Michaelis-Menten kinetics, then it is supposed that relative amounts of metabolites formed through saturation-controlled processes will *decrease* with an increase in dose. A quantitative discussion of metabolite bioavailability changes is not possible, however. The plasma bioavailability of a metabolite can change for at least three different reasons: (1) a variation in the formation rate, (2) a variation in the volume of distribution, and (3) a variation in the rate of excretion (or subsequent biotransformations). Currently, the only way to quantify metabolite pharmacokinetics depends on the availability of disposition data obtained by i. v. administration of the metabolite itself.

However, a *qualitative* examination can be carried out by discussing the ratio between the molecular-weight-corrected AUC values for the metabolites and the corresponding parameter for the parent drug (60 vs 120 mg/m^2: EPIol, 0.23 $\pm$ 0.10 vs 0.22 $\pm$ 0.06, $P = 0.218$; G1, 0.46 $\pm$ 0.14

vs 0.62 ± 0.40, $P = 0.631$; G2, 0.21 ± 0.05 vs 0.30 ± 0.16, $P = 0.218$; and 75 vs 150 mg/m^2: EPIol, 0.33 ± 0.22 vs 0.32 ± 0.19, $P = 0.218$; G1, 0.51 ± 0.23 vs 0.46 ± 0.17, $P = 0.68$; G2, 0.18 ± 0.10 vs 0.22 ± 0.10, $P = 0.68$). No statistically significant dose-dependent variation can be observed. In conclusion, all of the metabolic pathways seem well preserved when the dose is doubled, and there are no evident signs of "saturation kinetics."

Given the different shape of the concentration-time curve, care must be taken when the AUC values for the unchanged drug are compared with those for the metabolites. For instance, the EPI-G1 AUC ratio (molecular-weight-corrected) calculated for patient 1 was equal to 1.7 as measured during the 5-min to 24-h interval but was equal to 3.0 as measured from the start of the infusion to infinity.

In conclusion, the data collected in this work indicate that when the EPI dose was increased from 60 to 120 mg/m^2 in patients with normal liver and kidney functions, drug-dependent nonlinearity was completely absent. When the dose was increased from 75 to 150 mg/m^2, a trend toward nonlinear drug distribution as well as a consequent increase in peripheral bioavailability was observed in four of six patients. In these four patients, however, the EPI terminal half-life and the MRT did not significantly increase. Experimental EPI disposition after each treatment could be adequately described by a *linear* pharmacokinetic model. After 8/24 treatments, a nonlinear tissue-binding model gave a slightly better description of the experimental data. However, even in these cases, the deviation from linearity was of a very limited degree. Actually, only rather sophisticated plasma sampling and mathematical procedures are capable of detecting these deviations from linearity. We also reject a Michaelis-Menten nonlinearity. To quote a text-book notion, "If Michaelis-Menten kinetics are operative then one expects: (a) the percentage metabolized by the Michaelis-Menten path to decrease with an increase in dose; (b) the area under the concentration, time curve to increase more than proportionately with increases in dose and (c) semilogarithmic plots of blood levels to curve inwards" [24]. None of these conditions was satisfied in our patient sample.

References

1. Akaike H (1974) A new look at the statistical model identification. IEEE Trans Automat Contr 19: 716–723
2. Bevington PR (1970) Data reduction and error analysis for the physical sciences. McGraw-Hill, New York
3. Camaggi CM, Strocchi E, Tamassia V, Martoni A, Giovannini M, Iafelice G, Canova N, Marraro D, Martini A, Pannuti F (1982) Pharmacokinetic studies of 4′epidoxorubicin in cancer patients with normal and impaired renal functions and with hepatic metastases. Cancer Treat Rep 66: 1819–1824
4. Camaggi CM, Comparsi R, Strocchi E, Testoni F, Pannuti F (1988) HPLC analysis of doxorubicin, epirubicin and fluorescent metabolites in biological fluids. Cancer Chemother Pharmacol 21: 216–220
5. Camaggi CM, Comparsi R, Strocchi E, Testoni F, Angelelli B, Pannuti F (1988) Epirubicin and doxorubicin comparative metabolism and pharmacokinetics. Cancer Chemother Pharmacol 21: 221–228
6. Camaggi CM, Strocchi E, Carisi P, Martoni A, Tononi A, Guaraldi M, Strolin-Benedetti M, Efthymiopoulos C, Pannuti F (1992) Idarubicin metabolism and pharmacokinetics after intravenous and oral administration in cancer patients: a cross-over study. Cancer Chemother Pharmacol 30: 307–316
7. Cassinelli G, Configliacchi E, Penco S, Rivola G, Arcamone F, Pacciarini A, Ferrari L (1984) Separation, characterization and analysis of epirubicin (4′-epidoxorubicin) and its metabolites from human urine. Drug Metab Dispos 12: 4–20
8. Dixon WJ, Brown MB (1979) BMDP-79 biomedical computer programs. P-series. University of California Press, Berkeley
9. Draper N, Smith H (1966) Applied regression analysis. J Wiley, New York
10. Eadie WT, Drijard D, James FE, Ross M, Sadoulet B (1971) Statistical methods in experimental physics. North-Holland, Amsterdam
11. Eksborg S, Stendahl U, Lönroth U (1986) Comparative pharmacokinetics of Adriamycin and 4′-epi-Adriamycin after their simultaneous intravenous administration. Eur J Clin Pharmacol 30: 629
12. Freedman LS, Workman P (1988) When can the infusion period be safely ignored in the estimation of pharmacokinetic parameters of drugs in humans? Cancer Chemother Pharmacol 22: 95–103
13. Ganzina F (1979) 4′-Epidoxorubicin, a new analogue of doxorubicin: a preliminary overview of preclinical and clinical data. Cancer Treat Rev 10: 1–22
14. Gibaldi G, Perrier D (1982) Pharmacokinetics, 2nd edn. Marcel Dekker, New York
15. Goodyear MDE (1988) Do doxorubicin and its enantiomer 4′-epidoxorubicin have equivalent activity? A meta-analysis of randomized trials comparing two analogues. Proc Am Assoc Cancer Res 29: 192
16. Jakobsen P, Steiness E, Bastholt L, Dalmark M, Lorenzen A, Petersen D, Gjedde SB, Sandberg E, Rose C, Nielsen OS, Mouridsen HT, Jakobsen A (1991) Multiple-dose pharmacokinetics of epirubicin at four different dose levels: studies in patients with metastatic breast cancer. Cancer Res 28: 63–68
17. James F, Ross M (1983) MINUIT D506. Function minimization and error analysis. CERN Computer Centre Program Library, Geneva
18. Manaka RC, Schumitzky A, Wolf W (1981) Symbolic programs for structural identification of linear pharmacokinetic systems. Comput Methods Programs Biomed 13: 203–213
19. Moore JW, Pearson RG (1981) Kinetics and mechanism, 3rd edn. John Wiley & Sons, New York
20. Mross K, Maessen P, Vijgh WJF van der, Gall H, Boven E, Pinedo HN (1988) Pharmacokinetics and metabolism of epidoxorubicin and doxorubicin in humans. J Clin Oncol 6: 517–526
21. Perrier D, Mayersohn M (1982) Noncompartmental determination of the steady-state volume of distribution for any mode of administration. J Pharm Sci 71: 372–373
22. Robert J, Vrignaud P, Nguyen-Ngoc T, Iliadis A, Mauriac L, Hurteloup P (1985) Comparative pharmacokinetics and metabolism of doxorubicin and epirubicin in patients with metastatic breast cancer. Cancer Treat Rep 69: 633–640
23. Tjuljandin SA, Doig RG, Sobol MM, Watson DM, Sheridan WP, Morstyn G, Mihaly G, Green MD (1990) Pharmacokinetics and toxicity of two schedules of high dose epirubicin. Cancer Res 50: 5095–5101
24. Wagner JG (1979) Fundamentals of clinical pharmacokinetics. Drug Intelligence Publications, Hamilton, Ohio
25. Weenen H, Lenkelma JP, Penders PGM, McVie JG, Ten Bokkel Huinink WW, De Planque MM, Pinedo HM (1983) Pharmacokinetics of 4′-epi-doxorubicin in man. Invest New Drugs 1: 59–64
26. Yamaoka K, Nakagawa T, Uno T (1978) Application of Akaike's Information Criterion (AIC) in the evaluation of linear pharmacokinetic equations. J Pharmacokinet Biopharm 6: 165–175
27. Young CW (1984) Epirubicin: a therapeutically active doxorubicin analogue with reduced cardiotoxicity. In: Bonadonna G (ed) Advances in anthracycline chemotherapy: epirubicin. Masson Milan, pp 183–188
28. Young CW (1989) Clinical toxicity of epirubicin. In: Robustelli della Cuna G, Bonadonna G (eds) Update on epirubicin. Advances in clinical oncology, vol 2. Medico-scientifiche, Pavia, pp 29–38